Functionalization of Carbon Nanotubes by Electrochemical Reduction of Aryl Diazonium Salts: A Bucky Paper Electrode

Jeffrey L. Bahr, Jiping Yang, Dmitry V. Kosynkin, Michael J. Bronikowski, Richard E. Smalley, and James M. Tour*

Contribution from the Department of Chemistry and Center for Nanoscale Science and Technology, MS 222, Rice University, 6100 Main Street, Houston, Texas 77005

Received February 20, 2001. Revised Manuscript Received April 25, 2001

Abstract: Small-diameter (ca. 0.7 nm) single-wall carbon nanotubes are predicted to display enhanced reactivity relative to larger-diameter nanotubes due to increased curvature strain. The derivatization of these small-diameter nanotubes via electrochemical reduction of a variety of aryl diazonium salts is described. The estimated degree of functionalization is as high as one out of every 20 carbons in the nanotubes bearing a functionalized moiety. The functionalizing moieties can be removed by heating in an argon atmosphere. Nanotubes derivatized with a 4-*tert*-butylbenzene moiety were found to possess significantly improved solubility in organic solvents. Functionalization of the nanotubes with a molecular system that has exhibited switching and memory behavior is shown. This represents the marriage of wire-like nanotubes with molecular electronic devices.

Introduction

Since their discovery in 1991,[1] there has been a great deal of interest in derivatization of single-wall carbon nanotubes (SWNTs) to facilitate their manipulation, enhance their solubility, and make them more amenable to composite formation. Success at covalent sidewall derivatization of purified SWNTs has been limited in scope, and the reactivity of the sidewalls has been compared to that of the basal plane of graphite.[2] The only truly viable route to direct sidewall functionalization of purified SWNTs has been fluorination at elevated temperatures.[3] These functionalized nanotubes may either be de-fluorinated by treatment with hydrazine or allowed to react with strong nucleophiles, such as alkyllithium reagents.[4,5] Although fluorinated nanotubes may well provide access to a variety of functionalized materials, the two-step protocol and functional group intolerance to organolithium reagents make alternate routes worth developing. Other attempts at sidewall modification have been hampered by the presence of significant graphitic or amorphous carbon contaminants[6] or have required solubilization via chemistry on the ends of cut nanotubes.[7] A more accommodating and direct approach to functionalized nanotubes is therefore desirable.

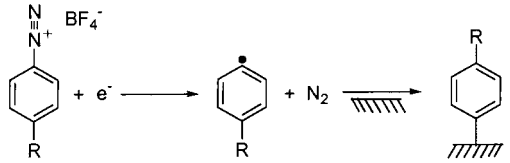

Figure 1. Electrochemical reduction of an aryl diazonium salt, giving a reactive radical that covalently attaches to a carbon surface, as in refs 10−14.

Aryl diazonium salts are known to react with olefins (Meerwein reaction[8]) and have also been shown to arylate aromatic compounds.[9] In solution-phase reactions, diazonium salt decomposition is typically catalyzed by a metal salt such as copper(I) chloride, giving a reactive aryl radical. In some cases, the reaction is believed to proceed through an aryl cation. This type of chemistry has been successfully applied to the modification of carbon surfaces via grafting of electrochemically reduced aryl diazonium salts.[10−14] Reduction gives an aryl radical that covalently attaches to the carbon surface, as shown in Figure 1. This technique has been applied to both highly ordered pyrolitic graphite (HOPG) and glassy carbon (GC) electrodes. Additionally, the theoretical aspects of energetic radical collisions with carbon nanotubes have been investigated and predicted to be a viable means of functionalization.[15]

* Corresponding author. Department of Chemistry and Center for Nanoscale Science and Technology-MS 222, Rice University, PO Box 1892, Houston, TX 77005. Fax: 713-348-6250. E-mail: tour@rice.edu.

(1) Iijima, S.; Ichihashi, T. *Nature* **1993**, *363*, 603−605.
(2) Aihara, J. *J. Phys. Chem.* **1994**, *98*, 9773−9776.
(3) Mickelson, E. T.; Huffman, C. B.; Rinzler, A. G.; Smalley, R. E.; Hauge, R. H.; Margrave, J. L. *Chem. Phys. Lett.* **1998**, *296*, 188−194.
(4) Boul, P. J.; Liu, J.; Mickelson, E. T.; Huffman, C. B.; Ericson, L. M.; Chiang, I. W.; Smith, K. A.; Colbert, D. T.; Hauge, R. H.; Margrave, J. L.; Smalley, R. E. *Chem. Phys. Lett.* **1999**, *310*, 367−372.
(5) Mickelson, E. T.; Chiang, I. W.; Zimmerman, J. L.; Boul, P. J.; Lozano, J.; Liu, J.; Smalley, R. E.; Hauge, R. H.; Margrave, J. L. *J. Phys. Chem. B* **1999**, *103*, 4318−4322.
(6) Chen, Y.; Haddon, R. C.; Fang, S.; Rao, A. M.; Eklund, P. C.; Lee, W. H.; Dickey, E. C.; Grulke, E. A.; Pendergrass, J. C.; Chavan, A.; Haley, B. E.; Smalley, R. E. *J. Mater. Res.* **1998**, *13*, 2423−2431.
(7) Chen, J.; Hamon, M. A.; Hu, H.; Chen, Y.; Rao, A. M.; Eklund, P. C.; Haddon, R. C. *Science* **1998**, *282*, 95−98.
(8) Obushak, M. D.; Lyakhovych, M. B.; Ganushchak, M. I. *Tetrahedron Lett.* **1998**, *39*, 9567−9570.
(9) Gadallah, F. F.; Elofson, R. M. *J. Org. Chem.* **1969**, *34*, 3335−3339.
(10) Delamar, M.; Désarmot, G.; Fagebaume, O.; Hitmi, R.; Pinson, J.; Savéant, J.-M. *Carbon* **1997**, *35*, 801−807.
(11) Allongue, P.; Delamar, M.; Desbat, B.; Fagebaume, O.; Hitmi, R.; Pinson, J.; Savéant, J.-M. *J. Am Chem. Soc.* **1997**, *119*, 201−207.
(12) Ortiz, B.; Saby, C.; Champagne, G. Y.; Bélanger, D. *J. Electroanal. Chem.* **1998**, *455*, 75−81.
(13) Saby, C.; Ortiz, B.; Champagne, G. Y.; Bélanger, D. *Langmuir* **1997**, *13*, 6805−6813.
(14) Delamar, M.; Hitmi, R.; Pinson, J.; Savéant, J. M. *J. Am. Chem. Soc.* **1992**, *114*, 5883−5884.
(15) Sinnott, S. B.; Ni, B. *Phys. Rev. B* **2000**, *61*, 343−346.

10.1021/ja010462s CCC: $20.00
Published on Web 06/14/2001

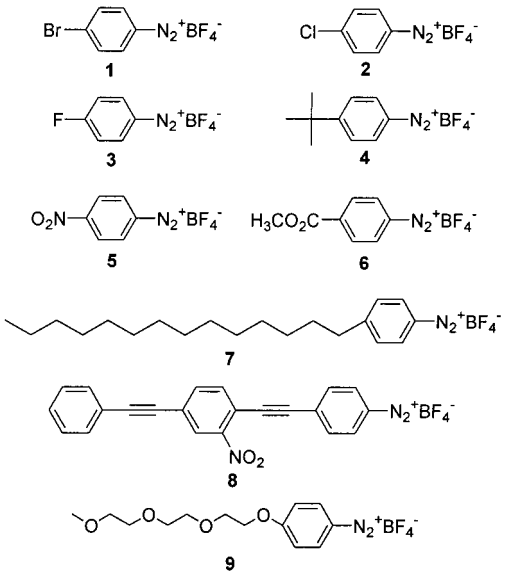

Figure 2. Aryl diazonium salts used to derivatize single-wall carbon nanotubes. Preparation and characterization of these salts is found in the Experimental Section.

Recently, a method for producing small-diameter (ca. 0.7 nm) single-wall carbon nanotubes was developed by Smalley et al.[16] As the diameter of these nanotubes is approximately the same as that of C_{60}, they are expected to display enhanced reactivity relative to the larger-diameter tubes typically produced by laser oven methods, since the reactivity of C_{60} has been attributed in part to curvature strain.[17,18] We report here the functionalization of these small-diameter nanotubes via electrochemical reduction of aryl diazonium salts, in a manner similar to that employed for functionalization of other carbon surfaces.[10−14] Although electrochemically induced reaction is the most favorable process, we also noticed that a thermal reaction is efficacious. A variety of diazonium salts have been used, including those that provide moieties conducive to further elaboration after attachment to the nanotubes. Also, an oligo(phenylene ethylene) molecular device similar to one that has been shown to exhibit memory and room-temperature negative differential resistance[19] has been attached to the nanotubes.

Results

Materials. The purified single-wall nanotube samples (hereafter, **SWNT-p**) used in this investigation contained little amorphous or other extraneous carbon contaminants (see Experimental Section for purification procedure). This fact is significant, as the presence of such material has hindered the ability to determine whether previous sidewall derivatization efforts were successful.[6] The residual iron content (catalyst from gas-phase growth technique) in the samples was ca. 0.3 atomic %. The diazonium salts used to derivatize **SWNT-p** are shown in Figure 2. Compounds **1**−**7** were prepared from the corresponding aniline derivatives using nitrosonium tetrafluoroborate. The synthesis of **8** has been previously reported.[20] Compound **9** was prepared according to Scheme 1. Characterization of these compounds is found in the Experimental Section. For the derivatization experiments, a piece of bucky paper, formed by filtration of a suspension, was used as the working electrode in a three-electrode cell and immersed in an acetonitrile solution containing the diazonium salt and an electrolyte. Reaction of the diazonium salts in Figure 2 with **SWNT-p** generated **SWNT-x**, where **x** is the functionalized phenyl moiety of diazonium salt **1**−**9**, respectively.

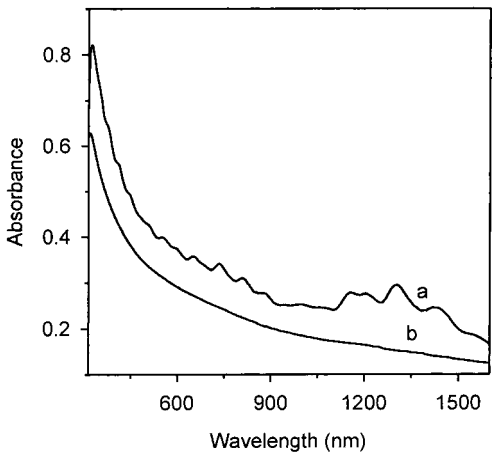

Figure 3. Absorption spectra in dimethylformamide, illustrating the loss of structure on functionalization; (a) pristine **SWNT-p**, (b) **SWNT-1**. The absorbance intensities have been adjusted to clarify the change in structure; there is no implication that derivatization lowers the base optical density throughout this region.

Scheme 1

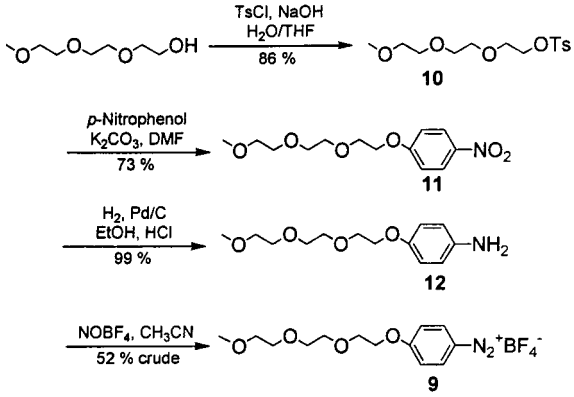

Characterization. The electronic structure and optical properties of single-wall carbon nanotubes have been investigated.[21−23] The UV/vis/NIR absorption spectra of **SWNT-p** and **SWNT-1** are shown in Figure 3. The features in the spectrum of **SWNT-p** are due to singularities in the density of states (DOS) and in this spectral region are attributed to the band gap transitions in semiconducting nanotubes. The width of these features is due to the overlap of features from tubes of different diameters and chiral indices. These transitions are no longer visible for **SWNT-1**, and the spectrum is essentially featureless. The absorption spectra of **SWNT-2**−**SWNT-7** are similar, with no apparent features. The spectra of **SWNT-8** (Figure 4) and **SWNT-9** retained some visible features, but these were significantly reduced relative to **SWNT-p**. The loss of structure

(16) Nikolaev, P.; Bronikowski, M. J.; Bradley, R. K.; Rohmund, F.; Colbert, D. T.; Smith, K. A.; Smalley, R. E. *Chem. Phys. Lett.* **1999**, *313*, 91−97.
(17) Haddon, R. C. *Science* **1993**, *261*, 545−549.
(18) Haddon, R. C. *J. Am. Chem. Soc.* **1997**, *119*, 1797−1798.
(19) (a) Chen, J.; Wang, W.; Reed, M. A.; Rawlett, A. M.; Price, D. W.; Tour, J. M. *App. Phys. Lett.* **2000**, *77*, 1224−1226. (b) Reed, M. A.; Chen, J.; Rawlett, A. M.; Price, D. W.; Tour, J. M. *App. Phys. Lett.* **2001**, *78*, 3735−3737.
(20) Kosynkin, D.; Tour, J. M. *Org. Lett.* **2001**, *3*, 993−995.
(21) Liang, W. Z.; Wang, X. J.; Yokojima, S.; Chen, G. H. *J. Am. Chem. Soc.* **2000**, *122*, 11129−11137.
(22) Jost, O.; Gorbunov, A. A.; Pompe, W.; Pichler, T.; Friedlein, R.; Knupfer, M.; Reibold, M.; Bauer, H.-D.; Dunsch, L.; Golden, M. S.; Fink, J. *App. Phys. Lett.* **1999**, *75*, 2217−2219.
(23) Wu, J.; Duan, W.; Gu, B.-L.; Yu, J.-Z.; Kawazoe, Y. *App. Phys. Lett.* **2000**, *77*, 2554−2556.

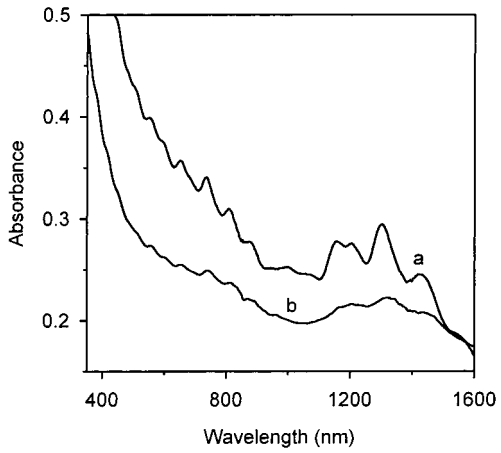

Figure 4. Absorption spectra in dimethylformamide; (a) **SWNT-p**, (b) **SWNT-8**.

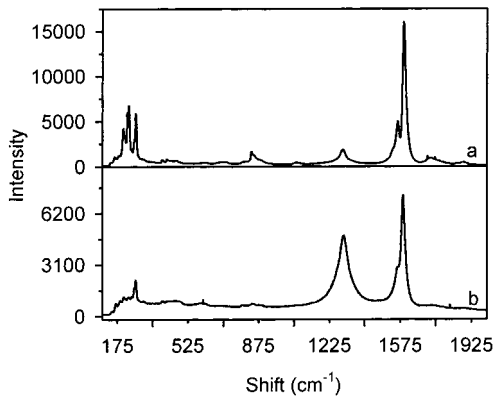

Figure 5. Raman scattering from pure and derivatized samples; (a) **SWNT-p**, (b) **SWNT-1**. Samples were pieces of bucky paper. Excitation was at 782 nm.

in the absorption spectra is indicative of significant electronic perturbation of the nanotubes and disruption of the extended π network. This effect is most consistent with covalent functionalization rather than simple adsorption to the nanotube walls or end caps.

Raman spectroscopy of single-wall carbon nanotubes is also well developed both theoretically and experimentally.[24−26] The Raman spectrum of **SWNT-p** (Figure 5) displays two strong bands: the so-called radial breathing ($\omega_r \approx 230$ cm^{-1}) and tangential ($\omega_t \approx 1590$ cm^{-1}) modes. The multiple peaks seen in the radial breathing mode are due to the distribution of tube diameters in the sample. The weaker band centered at ca. 1290 cm^{-1} is attributed to disorder (ω_d) or sp^3-hybridized carbons in the hexagonal framework of the nanotube walls. The minor band at 850 cm^{-1} is also characteristic of these small-diameter nanotubes, although its molecular origin is not clear. The spectrum of **SWNT-1** (Figure 5) is quite different. Most notably, the relative intensity of the disorder mode is much greater. This is also an expected result of the introduction of covalently bound moieties to the nanotube framework, wherein significant amounts of the sp^2 carbons have been converted to sp^3 hybridization. The Raman spectra of the other functionalized materials display similar modifications but to different degrees. The frequency of the disorder mode and the relative intensities of the three major bands are shown in Table 1. In all cases, there is no significant change in the frequency of the disorder mode, and the intensity of this mode increased relative to the intensity of the breathing and tangential modes. The intensity of the tangential mode is also increased relative to that of the radial breathing mode in most cases, and the overall intensity is lower. In some cases, Raman spectra collected after functionalization revealed changes in the relative intensities of the peaks within the radial breathing mode region. For example, the Raman spectra in this region are shown in Figure 6 for **SWNT-p** and **SWNT-4**. We did not observe changes in the Raman spectra that could be attributed to the functionalizing moieties. The presence of bands due to nitrophenyl moieties on modified GC electrodes has been detected by subtraction of untreated GC spectra, revealing several bands between 1100 and 1175 cm^{-1}.[27] However, the bands were quite weak and difficult to resolve, even though monolayer coverage with the nitrophenyl moiety was achieved. In the present case, the probable less extensive degree of functionalization or random orientation of the aryl appendages renders the direct detection of moieties on the nanotubes with Raman scattering exceedingly difficult. Their effect on the properties of the nanotubes is abundantly clear, however.

Infrared spectroscopy (FT-IR, ATR) was also used to characterize some of the derivatized materials. The spectrum of **SWNT-4** (Figure 7a) clearly shows significant C−H stretching from the *tert*-butyl moiety at ca. 2950 cm^{-1}. In the spectrum

Table 1. Disorder Mode Frequency and Intensity Ratios of Major Peaks in Raman Scattering Experiments

compd	ω_d	intensity ratio (ω_r:ω_d:ω_t)[a,b]
SWNT-p	1291	1.0:0.3:2.7
SWNT-1	1295	1.0:2.2:3.3
SWNT-2	1294	1.0:2.2:4.0
SWNT-3	1295	1.0:2.0:4.0
SWNT-4	1290	1.0:1.4:3.7
SWNT-5	1291	1.0:1.4:3.7
SWNT-6	1292	1.0:1.5:3.5
SWNT-7	1293	1.0:1.3:3.8
SWNT-8	1292	1.0:0.7:3.0
SWNT-9	1293	1.0:0.8:2.5

[a] ω_r = radial breathing mode, ω_d = disorder mode, ω_t = tangential mode. [b] ω_r intensity taken at 265 cm^{-1}; other intensities taken at maxima.

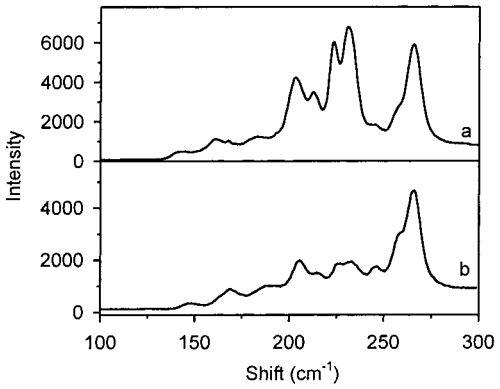

Figure 6. Raman spectra in the radial breathing mode region; (a) **SWNT-p**, (b) **SWNT-4**.

(24) Richter, E.; Subbaswamy, K. R. *Phys. Rev. Lett.* **1997**, *79*, 2738−2740.

(25) Rao, A. M.; Richter, E.; Bandow, S.; Chase, B.; Eklund, P. C.; Williams, K. A.; Fang, S.; Subbaswamy, K. R.; Menon, M.; Thess, A.; Smalley, R. E.; Dresselhaus, G.; Dresselhaus, M. S. *Science* **1997**, *275*, 187−191.

(26) Li, H. D.; Yue, K. T.; Lian, Z. L.; Zhan, Y.; Zhou, L. X.; Zhang, S. L.; Shi, Z. J.; Gu, Z. N.; Liu, B. B.; Yang, R. S.; Yang, H. B.; Zou, G. T.; Zhang, Y.; Iijimas, S. *App. Phys. Lett.* **2000**, *76*, 2053−2055.

(27) Liu, Y.-C.; McCreery, R. L. *J. Am. Chem. Soc.* **1995**, *117*, 11254−11259.

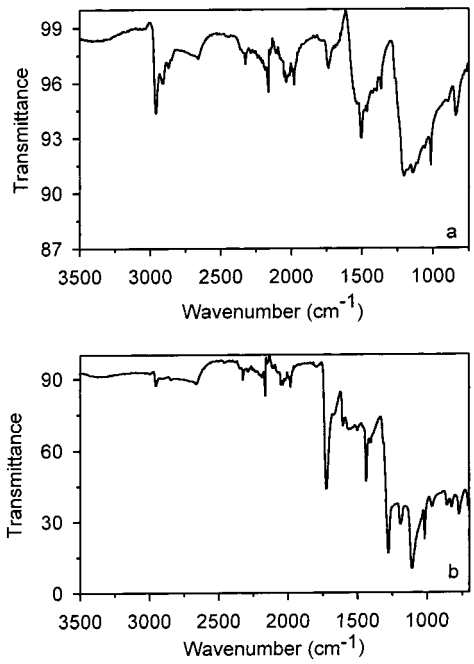

Figure 7. Infrared spectra (attenuated total reflectance) of derivatized nanotubes; (a) **SWNT-4**, (b) **SWNT-6**.

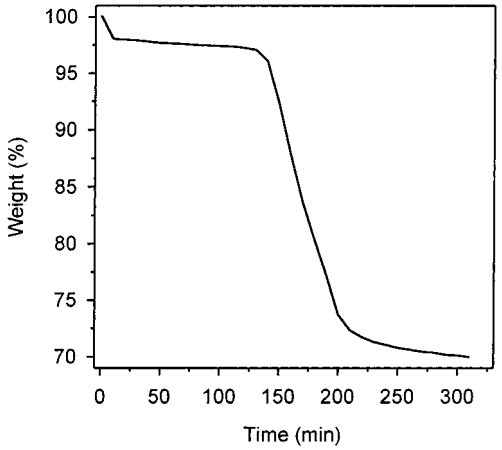

Figure 8. Thermogravimetric analysis data in argon. Temperature profile: 1 h hold at 150 °C, ramp 5 °C min^{-1} to 500 °C, 2.5 h hold at 500 °C.

of **SWNT-6** (Figure 7b), the carbonyl (C═O) stretch is apparent at 1731 cm^{-1} (1723 cm^{-1} in precursor diazonium salt), along with minor C−H stretching modes in the 2900 cm^{-1} region.

Electron microprobe analysis (EMPA) experiments revealed 2.7 atomic % chlorine, relative to 96.2 atomic % carbon, for **SWNT-2**. Similar experiments revealed 3.5 atomic % fluorine, relative to 94.5 atomic % carbon, for **SWNT-3**. These percentages correspond to estimated stoichiometries of $CR_{0.036}$ for **SWNT-2**, and $CR_{0.05}$ for **SWNT-3**, where C is a carbon in the nanotube framework, and R is the functionalizing moiety. In other words, approximately one out of every 20−30 carbons in the nanotube bears a functionalized phenyl moiety. For the remaining functionalized materials, either they do not contain an element conducive to quantitative determination, or no standard was available for calibration, as in the case of **SWNT-1**.

In thermogravimetric analysis (TGA) of **SWNT-2** (Figure 8), a total weight loss of ca. 30% was observed on heating to 500 °C. De-gassing and solvent evaporation at low temperatures account for approximately 3% of the loss. The majority of the weight loss occurs at temperatures >400 °C. After TGA of

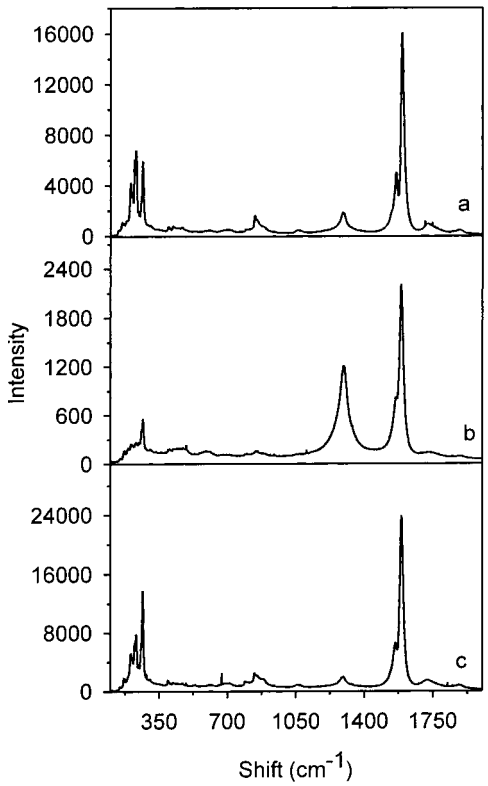

Figure 9. Raman spectra illustrating restoration of structure and relative mode intensities for **SWNT-2** after TGA; (a) **SWNT-p**, (b) **SWNT-2**, (c) **SWNT-2** after TGA.

Table 2. Weight Loss and Estimated Stoichiometries from TGA, with Heating to 500 °C in Argon

compd	observed % weight loss	stoicheometry ratio[a]
SWNT-p	5	NA
SWNT-1	35	1/25
SWNT-2	30	1/27
SWNT-3	26	1/20
SWNT-4	27	1/34
SWNT-5	26	1/31
SWNT-6	31	1/28
SWNT-7	39	1/36
SWNT-8	–	–
SWNT-9	36	1/40

[a] Nanotube carbons bearing a functionalized phenyl moiety. These values are compensated for weight loss at low temperatures due to solvent evaporation and degassing (ca. 2−4% in all cases).

SWNT-2, the Raman spectrum is restored to approximately that of **SWNT-p**, as seen in Figure 9. This restoration suggests removal of the functional moieties, leaving the nanotubes intact. The stoichiometry estimated from the EMPA data predicts a weight loss of ca. 25% in the case of such a removal. After accounting for weight loss due to solvent evaporation, these figures are in excellent agreement. The TGA and EMPA data for **SWNT-3** are also in good agreement. **SWNT-p** suffers only a ca. 5% weight loss following the same temperature profile. TGA data and estimated stoichiometries for the remaining materials (with the exception of **SWNT-8**; we did not prepare enough of this material for TGA) are shown in Table 2.

Analysis of the reaction products by scanning electron microscopy (SEM) did not reveal any visible evidence of functionalization or significant change from **SWNT-p**. Transmission electron microscopy (TEM) imaging of **SWNT-4**, however, revealed significant changes due to the functionalization. In images of **SWNT-p** (Figure 10a), the nanotube walls

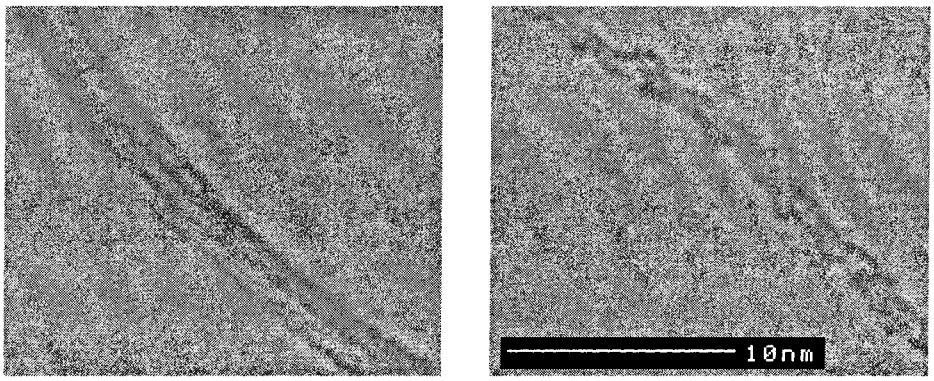

a b

Figure 10. Transmission electron microscopy images; (a) **SWNT-p**, (b) **SWNT-4**. Scale bar shown in (b) applies to (a) as well.

are essentially clean and uniform, and there is no overcoating of graphitic carbon. Images of **SWNT-4** (Figure 10b) revealed the presence of bumps on the sidewalls of the tubes, on the order of 2−6 Å in dimension. These bumps are seen on almost all individual tubes and on the exterior of ropes, although the resolution is not sufficient to see whether they are present on the walls of tubes buried within the ropes. These features are clearly a result of functionalization, but we cannot derive much information concerning the regioregularity of attachment to the tubes.

The solubility of single-wall carbon nanotubes is of significant interest to researchers in the field.[28−30] The three solvents most applicable for the underivatized small-diameter nanotubes are dimethylformamide, chloroform, and 1,2-dichlorobenzene.[28] **SWNT-4** was the only material found to offer significantly improved solubility in organic solvents. This material was even found to be somewhat soluble in tetrahydrofuran, as opposed to **SWNT-p** which had a complete lack of solubility for in this solvent. After sonication for about 30 min, the solution was found to contain approximately 50 mg L^{-1} of **SWNT-4**, with no visible particulate. After 36 h, some visible particulate was present, but the solvent was still almost black. This dark color was retained for at least several weeks. Solubility in dimethylformamide, chloroform, and 1,2-dichlorobenzene was also improved, with suspensions being formed much more rapidly than in the case of **SWNT-p**, and higher concentrations being achievable. This improvement in solubility is probably due to the blocking effect of the bulky *tert*-butyl group, which could inhibit the close contact necessary for "roping" of the nanotubes. **SWNT-5** and **SWNT-8** were found to be more soluble in dimethylformamide, but solubility in other solvents (tetrahydrofuran, toluene, 2-propanol, carbon disulfide, etc.) was not improved. **SWNT-9** was prepared in an effort to effect improved solubility in water and other hydrogen-bonding solvents. This functionalization, however, had quite the opposite result. We were not able to disperse the material in water or water containing 0.2% Triton X. We, in fact, encountered considerable difficulty in suspending the material in dimethylformamide, and other solvents did not even wet the material.

In an effort to assess the robustness of the functionalization and preclude simple intercalation or adsorption, we subjected **SWNT-1** to a variety of conditions involving additional sonication and heating. After these treatments, no discernible spectroscopic changes were observed. As an additional check, **SWNT-3** was reexamined by EMPA after additional sonication in acetonitrile, followed by filtration and washing. The fluorine content was 3.6 atomic %, as compared to 3.5 atomic % (vide supra), and hence within experimental limits

Discussion

Derivatization Mechanism. The functionalization described here is probably initiated in a manner similar to that shown in Figure 1. The aryl radical generated on reduction of the diazonium salts reacts with a nanotube, leaving an adjacent radical that may further react or be quenched by solvent. The propensity of the initial aryl radical to dimerize or abstract a hydrogen atom from the solvent is minimized by the fact that the radical is generated at the surface of the nanotube where reaction is desired. Indeed, herein lies the principal advantage of this method, as opposed to a solution-phase method in which the diazonium salt reduction is catalyzed by copper or some other metal. Since the nanotubes would be present in solution at quite low concentration, most aryl radicals would be disadvantageously quenched by some other species. Dimerization of nanotubes in the present case is also unlikely, due to lack of mobility in the solid state. A polymerization growth mechanism was proposed by McDermott et al.[31] for the derivatization of HOPG with 4-nitrophenyl diazonium salts. In McDermott's proposed mechanism, only a few aryl radicals attacked the carbon surface, and subsequent radicals attacked a growing chain of polyphenylene emanating from the original attack sites. The initial point of "nucleation" or reaction was considered to likely be a defect site. This locality of functionalization was investigated with spatially resolved Raman spectroscopy.[32] One may suggest a similar scenario in the present case, where only a few radicals become covalently attached to the SWNTs, and a growing polyphenylene chain wraps around the nanotubes. Polymer wrapping of nanotubes is known.[33−35] Alternatively, one may suggest polymerization of the diazonium salts in solution, followed by wrapping, with no actual covalent attachment to the nanotubes. Several factors

(28) Bahr, J. L.; Mickelson, E. T.; Bronikowski, M. J.; Smalley, R. E.; Tour, J. M. *Chem. Commun.* **2001**, 193−194.
(29) Ausman, K. D.; Piner, R.; Lourie, O.; Ruoff, R. S.; Korobov, M. *J. Phys. Chem. B* **2000**, *104*, 8911−8915.
(30) Niyogi, S.; Hu, H.; Hamon, M. A.; Bhowmik, P.; Zhao, B.; Rozenzhak, S. M.; Chen, J.; Itkis, M. E.; Meier, M. S.; Haddon, R. C. *J. Am. Chem. Soc*. **2001**, *123*, 733−734.
(31) Kariuki, J. K.; McDermott, M. T. *Langmuir* **1999**, *15*, 6534−6540.
(32) Ray, K.; McCreery, R. L. *Anal. Chem.* **1997**, *69*, 4680−4687.
(33) Dalton, A. B.; Stephan, C.; Coleman, J. N.; McCarthy, B.; Ajayan, P. M.; Lefrant, S.; Bernier, P.; Blau, W. J.; Byrne, H. J. *J. Phys. Chem.* **2000**, *104*, 10012−10016.
(34) Riggs, J. E.; Guo, Z.; Carroll, D. L.; Sun, Y.-P. *J. Am. Chem. Soc.* **2000**, *122*, 5879−5880.
(35) Tang, B. Z.; Xu, H. *Macromolecules* **1999**, *32*, 2569−2576.

argue against these events in the present case, however. First, polymer wrapping would not be a sufficient electronic perturbation to induce the spectroscopic changes seen in the derivatized materials.[35] Second, in the case of **SWNT-4**, polymerization after initial reaction with a nanotube would be severely inhibited by the steric bulk of the *tert*-butyl substituent. It is thus most likely that the functionalizations described here are the result of reaction at numerous sites on the nanotube sidewalls.

Unique "Bucky Paper" Issues. The use of bucky paper as a working electrode for the derivatization raises several issues. We did encounter reproducibility problems in the early stages of this investigation, and we have identified two factors that are critical to success. Electrical contact between the source and the bucky paper is of course critical. We found this difficulty alleviated by application of colloidal silver paste to the alligator clip used to hold the bucky paper. Additionally, the success of the reaction is somewhat dependent on the quality of the bucky paper. This perhaps hearkens to issue of sufficient electrical contact within the bucky paper itself. We have found that the quality of the paper is influenced by the quality of the suspension prior to filtration. Hence, it was helpful to achieve a suspension that contained little or no visible particulate prior to filtration. This condition ensures, macroscopically at least, a smooth, homogeneous paper that may have better electrical contact between the nanotube ropes and bundles that make up the bucky paper.

Degree of Functionalization. The characterization data suggest differing degrees of functionalization among the materials reported here. In Raman scattering, the most direct evidence lies in the relative intensity of the disorder mode peak at ca. 1290 cm^{-1}. Although no quantitative relationship between this ratio and the degree of substitution has been developed, the relationship is surely a direct one. The change in the relative ratio of the peaks in the radial breathing mode region (Figure 6) is also worthy of note. Since this Raman mode is resonance-enhanced, a lower intensity for a given-diameter nanotube may indicate a greater degree of functionalization for that particular-diameter nanotube. In other words, this observation may provide evidence for a greater reactivity of some tube diameters. Preferential interaction of polymers with certain tube diameters has been reported.[32] However, this effect is not consistent throughout the functionalized materials reported here. Additionally, it is the larger-diameter tubes (lower frequency shift) whose transitions are most significantly affected. This is not the situation one would expect in consideration of the predicted inverse relationship between the tube diameter and reactivity. The import of this observation is then not clear, and further investigation is required.

Total mass loss figures from the TGA experiments also indicate differing degrees of functionalization. Direct relation of this number to the degree of functionalization carries the caveat of assuming that all phenyl moieties are cleanly removed and that no other surface functionalities are lost. However, the good correlation between the mass loss and EMPA data for **SWNT-2** and **SWNT-3** suggest this is a reasonable assumption.

The UV/vis/NIR absorption spectra indicate a lower degree of functionalization for **SWNT-8** and **SWNT-9** but do not provide a true means for gauging the magnitude of the difference. As this technique probes the entire ensemble of species in solution, however, the spectra do suggest that the functionalizations in general are not merely a surface reaction, which would only change the spectroscopic properties of a smaller portion of the whole, dependent, of course, on the thickness of the bucky paper.

Some portion of the observed differences in the degree of functionalization is surely due to differences in reactivity of the salts. Such differences may give more or less opportunity for dimerization or otherwise disadvantageous quenching of the aryl radicals. A greater portion, however, is probably due to heterogeneity among the bucky paper electrodes, possibly in terms of defect frequency or diameter distribution within each bucky paper electrode. The lower degree of functionalization observed for **SWNT-8**, as evidenced by the Raman and absorption spectra, is due in part to a lower concentration of **8** in the reaction solution, necessitated by its poor solubility. In general, the solubility of the different salts at the liquid-surface interface region of the reaction may differ considerably. Finally, as previously mentioned, the quality of the bucky paper affects the success of the functionalizations in general. Hence, variance in this parameter accounts for some variation in the degree of functionalization.

Conclusions

Electrochemical reduction of aryl diazonium salts using a bucky paper electrode has been presented as a viable means of derivatization of small-diameter single-wall carbon nanotubes. Derivatization far beyond just the end caps is achieved, and the covalent attachment is quite robust. The series of diazonium salts used here give differing degrees of functionalization, although a single reason is not clearly responsible for these differences. With appropriately bulky moieties, solubility of the nanotubes in organic solvents can be significantly improved. The functionalizing moieties can be removed by heating to 500 °C in an argon atmosphere, restoring the pristine nanotubes. The functionalization technique described here is an enabling development that will permit modification of nanotubes to facilitate their incorporation into polymer composite materials and perhaps molecular electronic applications.

Experimental Section

Methylene chloride and acetonitrile were distilled from calcium hydride. Dimethylformamide was distilled and stored over molecular sieves. Tetrahydrofuran was distilled from sodium/benzophenone ketyl. All other reagents were obtained commercially and used without further purification. SEM experiments were performed at an accelerating voltage of 50 kV. Samples for TEM imaging were drop dried from THF onto a 200 mesh lacey carbon grid on a copper support. The accelerating voltage was 100 kV. Raman spectra were collected from solid samples, with excitation at 782 nm. UV/vis/NIR absorption spectra were collected in double-beam mode, with solvent reference. FT-IR spectra were collected using an attenuated total reflectance (ATR) accessory. TGA data were collected in argon. The instrument used for the EMPA experiments was calibrated, and data were taken from several different points on each sample ($\Delta d \approx 100\ \mu$M). The average of these points is reported in the Results section. NMR chemical shifts are reported in ppm downfield from TMS and referenced to solvent. Melting points are not corrected.

The small-diameter single-wall carbon nanotubes used in this investigation were produced by a gas-phase catalytic technique, using carbon monoxide as the feedstock and iron carbonyl as the catalyst.[16] The raw production material was purified by air oxidation at 150 °C for a period of 12 h, followed by annealing in argon at 800 °C for 1 h. Finally, this material was sonicated in concentrated hydrochloric acid (ca. 30 mg in 60 mL), filtered, washed extensively with water and 2-propanol, and dried under vacuum. The purity of these samples was verified by SEM, TEM, and EMPA.

General Procedure for Electrochemical Derivatization of SWNT-p. The apparatus used for the electrochemical derivatization experiments was a three-electrode cell, with $Ag/AgNO_3$ reference electrode and platinum wire counter electrode. A piece of bucky paper (1−2 mg) served as the working electrode. The bucky paper was

prepared by filtration of a 1,2-dichlorobenzene suspension over a 0.2 μM PTFE (47 mm, Sartorius) membrane. After drying under vacuum, the paper was peeled off the membrane, and a piece was excised for use in the derivatization. The bucky paper was held with an alligator clip that was previously treated with colloidal silver paste (Ted Pella, Inc.) and immersed in an acetonitrile solution of the diazonium salt (0.05 M for **SWNT-1**−**SWNT-7** and **SWNT-9**; 0.01 M for **SWNT-8**) and tetra-*n*-butylammonium tetrafluoroborate (0.05 M). Care was taken not to immerse the alligator clip itself. A potential of −1.0 V was applied for a period of 30 min. Care was taken for the exclusion of light, and nitrogen was bubbled through the solution during the experiment. After reaction, the portion of the "bucky paper" that was not immersed in the solution was excised, and the remainder was soaked in acetonitrile for 24 h and then washed with acetonitrile, chloroform, and ethanol. After drying, this material was sonicated in acetonitrile for 20 min, filtered, and washed again with acetonitrile, 2-propanol, and chloroform. The reaction products were dried under vacuum at room temperature prior to characterization. Control experiments without a diazonium salt confirm that these conditions do not affect the nanotubes, as verified by UV/vis/NIR, Raman, and TGA.

General Procedure for Diazotization of Aniline Derivatives. A portion of nitrosonium tetrafluoroborate (1.2 mol equiv) was weighed out in a glovebox and sealed. After removal from the glovebox, acetonitrile was added (3 mL/mmol of aniline), and the solution was cooled to −30 °C. A solution of the aniline derivative (1 mol equiv) in acetonitrile (ca. 1 mL/mmol) was added dropwise while stirring. In some cases, dry methylene chloride was used as a cosolvent for the aniline derivative (vide infra). After complete addition, stirring was continued for 30 min, at which time the cold bath was removed. After stirring for a total of 1 h, the solution was diluted with a 2× volume of ether and stirred. The precipitate was collected by filtration and washed with ether.

4-Bromobenzenediazonium tetrafluoroborate (1): yield 85%; mp 138 °C. ^{1}H NMR (400 MHz, CD_3CN) δ 8.22 (ABq, J = 9.1 Hz, $\Delta\nu$ = 102.1 Hz, 4 H).

4-**Chlorobenzenediazonium tetrafluoroborate (2):** yield 78%; mp 134 °C. ^{1}H NMR (400 MHz, CD_3CN) δ 8.24 (ABq, J = 9.2 Hz, $\Delta\nu$ = 214.2 Hz, 4 H).

4-**Fluorobenzenediazonium tetrafluoroborate (3):** yield 79%; mp 160 °C. ^{1}H NMR (400 MHz, CD_3CN) δ 8.64 (dd, J = 9.4, 9.5 Hz, 2 H), 7.69 (dd, J = 9.4, 9.5 Hz, 2 H).

4-***tert*-Butylbenzenediazonium Tetrafluoroborate (4).** The 4-*tert*-butylaniline was dissolved in a 1:1 mixture of acetonitrile and dry methylene chloride prior to addition to the nitrosonium tetrafluoroborate*:* yield 78%; mp 91 °C. IR (KBr) 3364.8, 3107.3, 2968.6, 2277.2, 1579.2, 1482.0, 1418.0, 1373.5, 1269.8, 1056.9, 841.1, 544.6, 621.4 cm^{-1}. ^{1}H NMR (400 MHz, CD_3CN) δ 8.16 (ABq, J = 9.0 Hz, $\Delta\nu$ = 298.7 Hz, 4 H), 1.30 (s, 12 H). ^{13}C NMR (100 MHz, CD_3CN) δ 168.85, 133.67, 130.43, 111.88, 37.86, 30.84.

4-Nitrobenzenediazonium tetrafluoroborate (5): yield 67%; mp 142 °C. ^{1}H NMR (400 MHz, CD_3CN) δ 8.72 (ABq, J = 9.4 Hz, $\Delta\nu$ = 65.4 Hz, 4 H).

4-Methoxycarbonylbenzenediazonium tetrafluoroborate (6): yield 80%; mp 113 °C. IR (KBr) 3103.8, 3042.4, 2955.3, 2294.7, 2310.1, 1731.4, 1582.9, 1439.5, 1306.4, 1045.23, 953.1, 860.9, 758.5, 666.3, 528.0 cm^{-1}. ^{1}H NMR (400 MHz, CD_3CN) δ 8.51 (ABq, J = 9.1 Hz, $\Delta\nu$ = 77.9 Hz, 4 H), 3.97 (s, 3 H). ^{13}C NMR (100 MHz, CD_3CN) 165.02, 142.44, 134.12, 133.16, 119.77, 54.53.

4-Tetradecylbenzenediazonium Tetrafluoroborate (7). The 4-tetradecylaniline was dissolved in a 1:1 mixture of acetonitrile and dry methylene chloride prior to addition to the nitrosonium tetrafluoroborate: yield 69%; mp 82 °C. IR (KBr) 3103.8, 2919.5, 2289.6, 1577.8, 1473.7, 1070.8, 1024.8, 844.5, 813.8, 716.9, 541.0, 510.2 cm^{-1}. ^{1}H NMR (400 MHz, $CDCl_3$) δ 8.02 (ABq, J = 8.8 hz, $\Delta\nu$ = 370.6 Hz, 4 H), 2.76 (t, J = 7.7 Hz, 2 H), 1.61 (quin, J = 7.8 Hz, 2 H), 1.23 (s, 22H), 0.85 (t, J = 7.0 Hz, 3 H). ^{13}C NMR (100 MHz, $CDCl_3$) δ 159.92, 133.26, 131.94, 110.96, 37.49, 32.34, 30.87, 30.12, 30.10, 30.07, 30.04, 29.91, 29.78, 29.75, 29.72, 23.11, 14.55.

2-(2-(2-Methoxyethoxy)ethoxy)ethyl *p*-Toluenesulfonate (10). Sodium hydroxide (3.65 g, 91.3 mmol) and tri(ethylene glycol)monomethyl ether (10.0 g, 60.9 mmol) were dissolved in a mixture of tetrahydrofuran and water (140 mL, 20 mL respectively). The solution was cooled in an ice bath. A solution of *p*-toluenesulfonyl chloride (12.76 g, 67.0 mmol) in 20 mL of tetrahydrofuran was added slowly. The solution was stirred at 0 °C for 3 h and then poured into 50 mL of ice water. The mixture was extracted several times with methylene chloride. The combined organic layers were washed with dilute HCl and then brine and dried over magnesium sulfate. After filtration, the solvent was removed by distillation at reduced pressure to give 16.6 g of the product (86% yield). IR (neat) 3503.3, 2878.5, 1597.9, 1453.1, 1356.3, 1292.0, 1247.0, 1177.2, 1097.5, 1019.0, 924.17, 818.0, 776.9, 664.5 cm^{-1}. ^{1}H NMR (400 MHz, $CDCl_3$) δ 7.50 (ABq, J = 7.9 Hz, $\Delta\nu$ = 179 Hz, 4H), 4.09 (app t, J = 4.8 Hz, 2H), 3.61 (app t, J = 4.9 Hz, 2H), 3.55 to 3.52 (m, 6H), 3.47 to 3.46 (m, 2H), 3.30 (s, 3H), 2.38 (s, 3H). ^{13}C NMR (100 MHz, $CDCl_3$) δ 145.21, 133.28, 130.21, 128.28, 72.20, 71.00, 70.85, 69.69, 68.95, 68.26, 59.31, 21.96.

4-(2-(2-(2-Methoxyethoxy)ethoxy)ethyl)nitrobenzene (11). A portion of **10** (9.0 g, 28.3 mmol) was dissolved in 50 mL of dimethylformamide. Potassium carbonate (11.75 g, 85.0 mmol) and 4-nitrophenol (3.82 g, 27.5 mmol) were added. The solution was stirred at 80 °C for 16 h. After cooling to room temperature, the solution was poured into water and extracted three times with methylene chloride. The combined organic layers were washed with water and then brine, dried over magnesium sulfate, and filtered, and the solvent was removed by distillation at reduced pressure. Chromatography (silica, hexane:ethyl acetate, 1:2) was employed to isolate the product (5.71 g, 73% yield). IR (neat) 3109.2, 3078.2, 2878.5, 1726.3, 1588.1, 1511.2, 1337.1, 1106.7, 1050.3, 932.6, 845.5, 753.3, 656.1 cm^{-1}. ^{1}H NMR ($CDCl_3$) δ 8.07 (d, J = 9.3 Hz, 2 H), 6.88 (d, J = 9.3 Hz, 2 H), 4.12 (app t, J = 4.8 Hz, 2 H), 3.79 (app t, J = 4.6 Hz, 2 H), 3.62 (m, 2 H), 3.58 to 3.53 (m, 4 H), 3.44 to 3.42 (m, 2 H), 3.26 (s, 3 H). ^{13}C NMR (100 MHz, $CDCl_3$) δ 164.29, 141.93, 126.24, 114.99, 72.29, 71.29, 71.03, 70.98, 69.77, 68.60, 59.44.

4-(2-(2-(2-Methoxyethoxy)ethoxy)ethyl)aniline (12). A portion of **11** (5.77 g, 20.2 mmol) was dissolved in 40 mL of acidic ethanol, and a catalytic amount of 10% palladium on carbon was added. The mixture was hydrogenated on a Parr apparatus (60 psi, 70 °C) for 3 h. The mixture was then filtered over Celite, washing with ethanol. Solid sodium bicarbonate was added, and the mixture was stirred for 2 h and then filtered. The solvent was removed by distillation at reduced pressure, leaving a brown oil (5.0 g, 98% yield). IR (neat) 3441.8, 3349.6, 2893.9, 2238.4, 1634.4, 1516.4, 1449.8, 1234.7, 1101.6, 907.0, 722.6 cm^{-1}. ^{1}H NMR (400 MHz, $CDCl_3$) δ 6.65 (ABq, J = 8.7 Hz, $\Delta\nu$ = 51.5 Hz, 4 H), 4.01 (t, J = 5.4 Hz, 2 H), 3.77 (t, J = 4.6 Hz, 2 H), 3.69 (app t, J = 5.6 Hz, 2 H), 3.65 to 3.59 (m, 4 H), 3.51 (app t, J = 4.9 Hz, 2 H), 3.34 (s, 3 H), 3.0 (brs, 2 H). ^{13}C NMR (100 MHz, $CDCl_3$) δ 152.30, 140.58, 116.75, 116.24, 72.31, 71.14, 71.02, 70.93, 70.30, 68.49, 59.44.

4-(2-(2-(2-Methoxyethoxy)ethoxy)ethyl)benzenediazonium Tetrafluoroborate (9). Compound **12** was subjected to the procedure described above for diazotization. The product was not crystalline, but rather a dark red, sticky material that was difficult to manipulate. The residue was mixed three times with ether, decanting the solvent. This material was sufficiently pure by ^{1}H NMR and was used without further purification or characterization (2.17 g, 52% yield). ^{1}H NMR (400, MHz, acetone-d_6) δ 8.12 (ABq, J = 9.5 Hz, $\Delta\nu$ = 479.5 Hz, 4 H), 4.53 (app t, J = 4.5 Hz, 2 H), 3.92 (t, J = 4.4 Hz, 2 H), 3.68 to 3.66 (m, 2 H), 3.61 to 3.56 (m, 4 H), 3.46 (t, J = 5.4 Hz, 2 H), 3.27 (s, 3 H).

Acknowledgment. Ivana Chiang and Professor John L. Margrave purified the raw SWNT material. The financial support of NASA (NASA-JSC-NCC 9-77, OSR 99091801), the NSF (NSR-DMR-0073046) and DARPA/ONR is gratefully acknowledged.

JA010462S